Korean J. Chem. Eng., 40(7), 1804-1814 (2023)
DOI: 10.1007/s11814-023-1400-8

pISSN: 0256-1115
eISSN: 1975-7220

A practical approach for kinetic analysis of hydrogenation of complex mineral base oil

Siddharth Modi*, Anand Kumar Tiwari*, Meka Srinivasa Rao*,†, Thummalapalli Snigdha, Thummalapalli Saritha**, Thummalapalli Chandra Sekhara Manikyam Gupta**, and Ajay Kumar****

*Department of Chemical Engineering, Dharmsinh Desai University, Nadiad, India
**Research and Development Centre, APAR Industries Ltd., Mumbai, India
(*Received 21 April 2022 • Revised 13 February 2023 • Accepted 17 February 2023*)

Abstract−The mineral base oil contains paraffins, naphthenes and aromatic hydrocarbons (AH) with carbon chains ranging from C_{14} to C_{60}. The presence of AH in base oil affects the performance of the product in many industrially oriented applications. The base oil considered in this work had AH around 14% w/w that needed to be reduced below 5% w/w for some applications and ideally 0% w/w. This paper demonstrates the practical approach for hydrogenation of complex mineral base oil for reducing AH. The mineral base oil rich in C_{20} was taken as the representative component. The hydrogen solubility in the oil was estimated using NRTL model. The semi-batch hydrogenation experiments were performed at different conditions and conversion of AH as high as 79% (i.e. 3% w/w) could be achieved. A second-order pseudo-homogeneous reaction kinetic model was proposed and validated. The conditions for reaction kinetics were optimized to achieve desirable conversion using Aspen Plus. To develop a continuous process for hydrogenation of AH, experiments were performed in a lab scale fixed bed reactor and the applicability of the kinetic model was validated. The kinetics was observed to be free of internal and external mass transfer limitations under lab scale conditions.

Keywords: Hydrogen Solubility, Kinetic Analysis, Semi-Batch Optimisation, Lab Scale Continuous FBR, Validation of Kinetic Model

INTRODUCTION

Mineral base oils are refined petroleum-based heavy hydrocarbons containing a complex mixture of paraffins, naphthenes, and aromatic hydrocarbons (AH). The mineral base oil has typical carbon distribution ranges between C_{14} to C_{60} with a boiling range of 250 °C to 650 °C [1-3]. They have a wide variety of applications, such as medicinal grade technical white oil, metal cutting or grinding fluid, hydraulic fluid, lubricating oil, circulating oil, coolant or thermic fluid in equipment like transformers [1,2,4]. Mineral base oils are widely used in transformers because of having very low electrical conductivity and are effective as coolants where it is called transformer oil. In these applications, mineral base oils are used with some additives and they are chemically treated to improve the application-specific properties. The desirable properties in the transformer oil are higher oxidation, UV, chemical and thermal stability along with improving dielectric constant by reducing the aromatic content [5]. The work presented in this paper primarily focuses on the chemical treatment of speciality mineral base oil for making it suitable as circulating oil and transformer oil.

The base oil is classified into five broad categories as per the API 1509, Appendix-E [6]. To meet the statutory requirements of API 1509 and market demand, the traditional base oil handling industries treat the aromatic rich oils with hot oleum to remove the undesirable unsaturates. Moreover, the oleum treatment process results in hazardous waste generation, and disposal of process waste is also an issue from the point of environmental regulations. Therefore, the European Union has issued strict guidelines for a labelled warning on all the derived products of mineral base oil treated by oleum [7]. Such stringent practices have discouraged the hot oleum treatment by exploring alternative routes like adsorption over acid clays or polymeric resins [8,9] or mild hydrogenation using alumina-based nickel (Ni) catalyst [10,11].

To address this, a mild hydrogenation using Ni catalyst to convert the aromatics to polycyclic paraffins (naphthenes) was taken up in this work. The untreated mineral base oil was selected for having potential application as circulating oil, and transformer oil has aromatic content in the range of 14% (±0.2%) on w/w basis, which is required to be below 5% w/w and ideally 0%.

The overall objective of the work was to develop a process for continuous hydrogenation of specialty mineral base oil to reduce AH below 5% w/w and ideally 0%. To achieve this, work was divided into the following four major steps. The first step is to decide a feasible region for experimentation by estimating the solubility of hydrogen in selected base oil having aromatic content of 14% on w/w. The second step is to develop a reaction kinetic model based on the data obtained from the semi-batch experiments conducted during this study and optimization of the operating conditions to maximize the conversion. The third step is to perform continuous experiments at lab scale and check the applicability of the developed kinetic model. The last step is to perform pilot-scale continuous experiments to develop an industrial-scale reactor and perform a detailed safety evaluation of the process.

Out of the four steps mentioned above, the first three steps, *i.e.*,

†To whom correspondence should be addressed.
E-mail: msrao@ddu.ac.in

feasible region for experimentation based on solubility, developing a working reaction kinetic model along with optimization of the operating conditions and validation of developed kinetic model on the lab-scale Fixed Bed Reactor (FBR) are of prime interest and discussed in this paper. A detailed study for development of continuous reactor and process is not in the scope of this paper.

The major constraints involved in this study are as follows: (1) Variable feed - the speciality base oil feed is industrial grade and its composition is variable; (2) Limited information - as the exact composition of the feed is not available except for the carbon distribution and overall mass composition of aromatics, naphthenes and paraffins; (3) Less concentration gradient - since the aromatics in the feed are around 14% (±0.2%) on w/w and required to be less than 5% on w/w basis, the overall reaction may be slow; (4) Physical constraint - the physical constraint of the experimental setup at lab scale, which may not allow to operate beyond the temperature 250 °C and pressure 80 bar in semi-batch mode and 500 °C and 40 bar in continuous mode; (5) Lack of literature - limited information is available on such speciality base oil and the issues associated with it in the open text except for few relevant patents on the similar grade of products [12-20]. The three steps (out of the four planned steps) were executed and demonstrated in this paper by duly considering the constraints involved in the study.

This paper is structured as follows. The characteristics of catalyst and feed, details of the experimental setup and analysis of product are mentioned in section 2. Section 3 elaborates the kinetic experiments in the feasible region, intra-particle diffusion limitations using Weisz-Prater Criterion (C_{WP}) and subsequent kinetic modelling. The parameter sensitivity analysis using Pearson product moment correlation coefficient (PPMCC) and kinetic optimization of operating conditions are discussed in section 4. Section 5 validates the applicability of the developed kinetic model on lab-scale continuous FBR. The significant findings and conclusions are discussed in section 6.

Table 1. Alumina-based Ni catalyst properties

Catalyst properties	Values
Ni (% w/w)	21
Nominal size (mm)	1.2
BET surface area (m^2/g)	112
Mean pore volume (cm^3/g)	0.43
Mean pore diameter (nm)	45
Bulk density (kg/m^3)	770

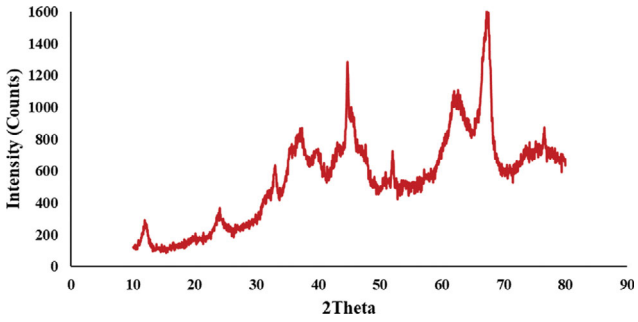

Fig. 1. XRD spectra of Ni catalyst.

EXPERIMENTAL SECTION

1. Physico-chemical Properties of Catalyst

The commercial Ni catalyst in the form of trilobe shaped 1.2 mm extrudates containing 21% Ni (w/w) as nickel oxide supported on porous alumina was used to study the kinetics of hydrogena-

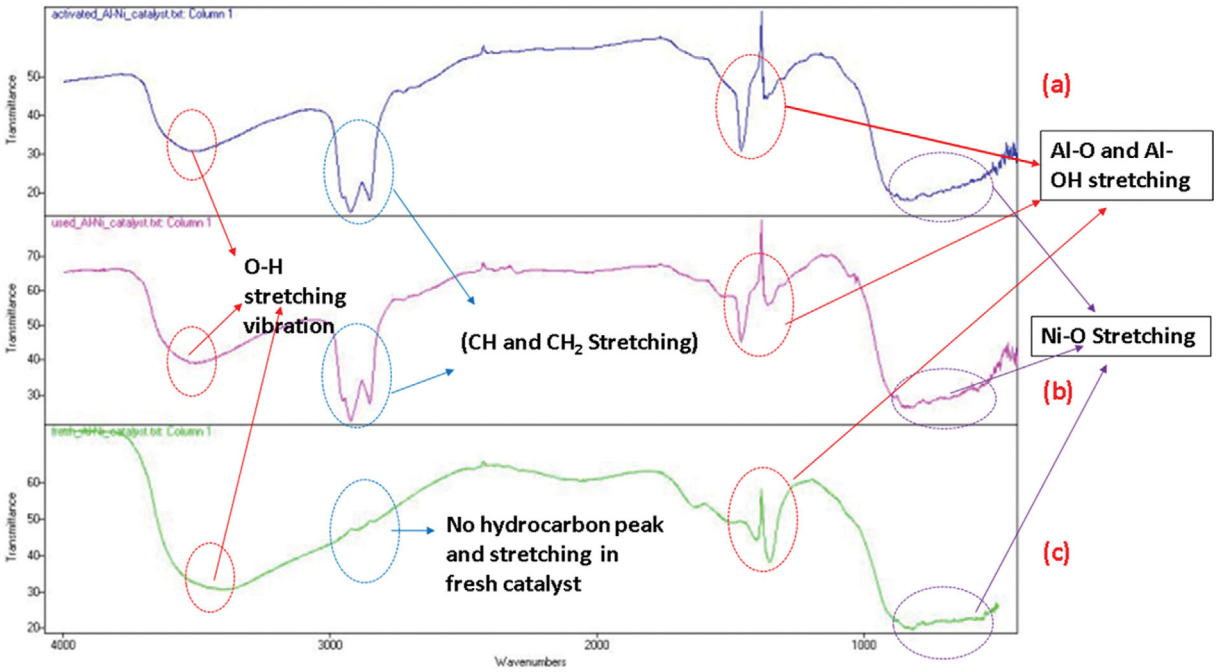

Fig. 2. FTIR spectra of Ni catalyst (a) activated Ni catalyst (b) used Ni catalyst (c) fresh Ni catalyst.

tion of complex mineral base oil. Further information of the Ni catalyst is reported in Table 1.

The physico-chemical properties of the Ni catalyst were analyzed using X-Ray diffraction (XRD) and Fourier transform infrared (FTIR) techniques. The 2θ peak observed in Fig. 1 at 37.00° and 45.35° confirms the presence of $NiAl_2O_4$ [21,22]. The 2θ value of 44.7°, 62.52° and 76.5° identifies the NiO [23-27]. The 2θ value at 32.95° suggests the possibility Ni_2O_3, whereas the 2θ value at 52.02° suggests the presence of Ni [28,29]. The 2θ values of 35.5°, 45.3°, 52.03° and 65.3° indicate the γ-Al_2O_3 [25,26,30].

The FTIR spectra of activated Ni catalyst, used Ni catalyst and fresh Ni catalyst are reported in Fig. 2(a)-(c), respectively. The NiO stretching is observed in all three Ni catalyst spectra between 850-400 cm^{-1}. Similar NiO stretching was observed by Sharma et al. [28]. The Al-O and Al-OH stretching is observed in all three Ni catalyst spectra in range of 1,600-1,300 cm^{-1}, which is also reported by Khodadadi et al. [26]. The CH and CH_2 stretching is observed in range of 3,000-2,800 cm^{-1} in both the activated Ni catalyst (Fig. 2(a)) and the used Ni catalyst (Fig. 2(b)). Such stretching is not observed in the fresh Ni catalyst (Fig. 2(c)). The bond stretching similar to Fig. 2(a)-(b) is reported by Kumar et al. for lubricating oil [31]. The O-H stretching is observed by Kremer et al. [32] in range of 3,600-3,300 cm^{-1}, which is also clearly visible in Fig. 2(a)-(c).

2. Chemicals

The mineral base oil used as the feed was industrial grade and it was provided by APAR Industries Limited, Mumbai. The overall composition of feed was observed to be 14% aromatics, 38.5% naphthenes and 47.5% paraffins by weight all ranging from C_{14} to C_{60}. The boiling point mass distribution as per ASTM D6352 [33] suggests that major carbon distribution in the feed is between C_{14} to C_{24} in which C_{20} has major fraction as shown in Fig. 3. The C_{20} contains naphthenes, paraffins and AH. The C_{20} AH has 26 different variants as reported in NIST data base [34]. Perylene is obtained to be maximum amongst all C_{20} AH in the petroleum isolates as reported by National Research Council (US) Committee on Perylene and analogues [35]. Hence, in this study we have considered C_{20} AH (Perylene) as the representative component for the AH hydrogenation. The average properties of the mineral base oil feed from four different batches are given in Table 2.

In addition to mineral base oil feed, other chemicals used in the experimentations were an inert oil, nitrogen and hydrogen gas. The

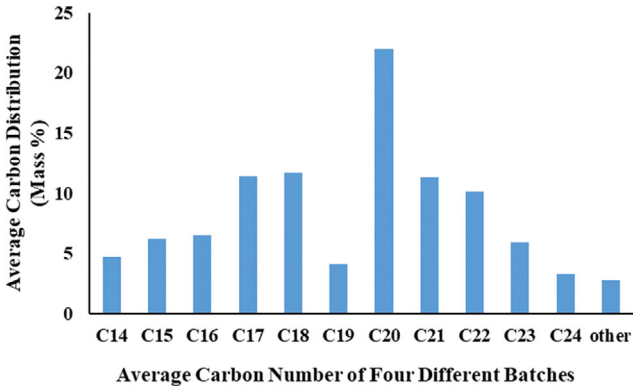

Fig. 3. %Mass distribution of carbon in mineral base oil.

Table 2. Average property and composition of the base oil feed

Average oil property (4 different batches)	Value
Initial Boiling Point (IBP), °C	200
End Boiling Point (EBP), °C	400
Specific Gravity, s_g	0.866
Viscosity Index (VI)	71
Pour Point, °C	−21
Aniline Point, °C	78
Flash Point (FP using close cup method), °C	145
Aromatics (% w/w)	14
Naphthenes (% w/w)	38.5
Paraffins (% w/w)	47.5

aromatics free inert oil was used to activate the Ni catalyst by removing the oxides from the catalyst surface. The inert oil was API group-II and it was completely saturated and sulfur-free to avoid any catalyst poisoning. The viscosity index of inert oil was 103 with a specific gravity of 0.87 and a close cup flash point of 256 °C. The ultra-pure grade nitrogen gas was used for the purging purpose and to identify the potential leakages in the system. The high purity hydrogen gas was used for the activation of the Ni catalyst and for the hydrogenation of mineral base oil feed.

3. Experimental Setup and Procedure

The kinetic experiments were carried out in an autoclave under semi-batch mode by continuously passing hydrogen through the liquid pool of base oil. The autoclave was made of SS-316 grade having a volume of 750 mL with provision for adjustable stirring in the range of 100 to 1,500 rpm (±2 rpm). The autoclave was designed to run at a maximum temperature of 250 °C (±1 °C) and a pressure of 80 bar (±0.1 bar).

Before the experiments were performed, the autoclave was purged for 2-3 hours by passing the nitrogen at 130 °C and 5 bar pressure to ensure the oxygen-free and moisture-free condition. The commercial Ni catalyst requires activation before use, which was achieved by reducing the catalyst using the aromatic free inert oil and hydrogen gas at 130 °C and 7 bar pressure for minimum of 5 hours. The Ni catalyst was filtered after its activation and used for hydrogenation. The kinetic experiments were performed using 450 gm of feed having AH of around 14% (±0.2%) w/w. The rotor speed in the autoclave was fixed to 500 rpm for kinetic study, except for the validation runs to check the effect of RPM on external mass transfer limitations.

4. Analytical Methods

The primary focus of the study was to bring the overall AH content of the feed below 5% w/w from the initial concentration of 14% w/w. The AH content along with paraffins and naphthenes was measured throughout the study using FTIR analysis as per BIS 13155 [36]. The FTIR spectra were recorded using a Perkin-Elmer spectrometer equipped with XT-KBr beam splitter and utilizing a DTGS TEC detector in the region of 4,000-400 cm^{-1} with 4 cm^{-1} spectral resolution and 36 kHz scanning speed. The aromatics, paraffins and naphthenes content in the mineral base oil was calculated from the FTIR analysis as per BIS 13155 using the following, Eqs. (1) to (4).

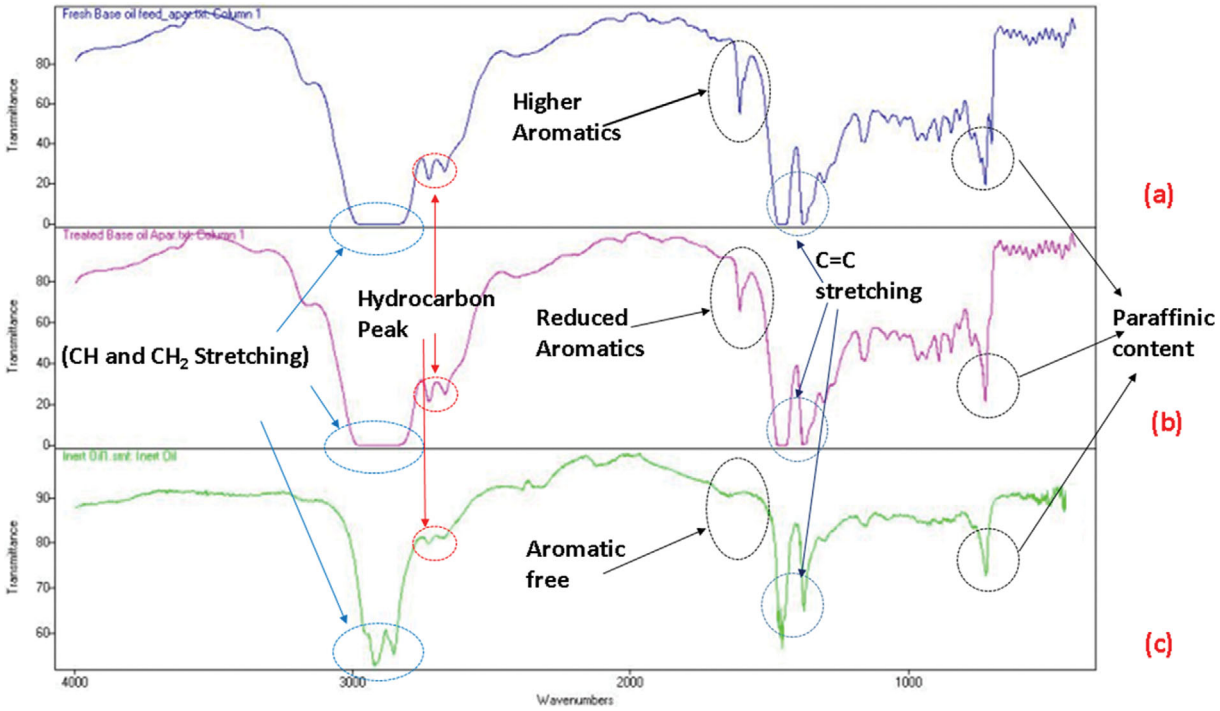

Fig. 4. FTIR spectra of mineral base oil and inert oil (a) fresh base oil (b) hydro-treated base oil (c) aromatic free inert oil.

Aromatic content (C_A) in the range of 1,650-1,550 cm^{-1}.

$$A = \frac{\log\left(\frac{I_0}{I}\right)}{C \times d} \quad (1)$$

$$C_A = 1.2 + 9.8(A) \quad (2)$$

where, A is the absorbance, C is the concentration factor (taken as 1 for undiluted oils) and d is the path length of cell in mm.

Paraffinic content (C_P) in the range of 750-680 cm^{-1}.

$$C_P = 29.9 + 6.6(A) \quad (3)$$

The naphthenic content (C_N) is calculated by subtracting the C_A and C_P from 100 as per BIS 13155 standard.

$$C_N = 100 - (C_A + C_P) \quad (4)$$

A typical FTIR spectrum of mineral base oil and aromatic free inert oil is reported in Fig. 4(a)-(c). The paraffinic content is clearly visible in all three oil samples in range of 750-680 cm^{-1} [36]. An intense aromatic peak is observed in fresh mineral base oil, which is reduced in intensity in hydro-treated oil and absent in the inert oil in range of 1,650-1,550 cm^{-1} [36]. The C=C stretching (1,500-1,300 cm^{-1}), CH and CH_2 stretching (3,000-2,800 cm^{-1}) and hydrocarbon peak (2,750-2,650 cm^{-1}) are comparable with lubricating base oil [31].

5. Necessary Safety Precautions

Since hydrogen is colorless and odorless with inherent explosive nature, it demands a certain level of safety precautions while handling. The hydrogen sensor was adopted while performing the experiments with a lower detectable set range of 10 ppm and an alarm set at 50 ppm and above. The Dow Fire and Explosion Index (F&EI) was calculated to be more than 240, exceeding the reference value of 159, which suggests that the degree of hazard is under the severe category [1,37]. More details on Dow F&EI, hazard operability study, fault tree and Bayesian analysis can be accessed through our past work [1,38].

RESULTS AND DISCUSSION

1. Feasible Condition for Experimentation

To determine the feasible region for performing experiments in liquid-phase, an estimation of hydrogen solubility in the base oil mixture is absolutely necessary. Since the feed base oil is highly variable in composition with evenly carbon distribution between C_{14} to C_{24} and dominated by C_{20} molecule, the following assumptions were made. (1) The feed oil having C_{14}-C_{24} carbon was represented as C_{20} molecule as the distribution is quite evenly balanced on either side. (2) In absence of exact information of detailed composition of feed, an average of four representative batches were taken with 14% (w/w) of $C_{20}H_{12}$ (Perylene) as AH, 38.5% (w/w) $C_{20}H_{40}$ (tetradecyclohexane) as naphthene and 47.5% (w/w) $C_{20}H_{42}$ (Eicosane) as paraffin.

The solubility of hydrogen in the assumed composition was estimated using Soave-Redlich-Kwong (SRK) and non-random two-liquid (NRTL) model using ASPEN Plus. The SRK model is preferred while dealing with hydrocarbon systems, and NRTL model is used when gas is assumed to be completely dissolved as a liquid. The ASPEN results suggested that both the models were estimating almost similar range of values for hydrogen solubility with a variation of less than 0.1%. The solubility of hydrogen was found to be increasing with an increase in temperature and pressure, which was reported and explained by Krichevsky-Ilinskaya and

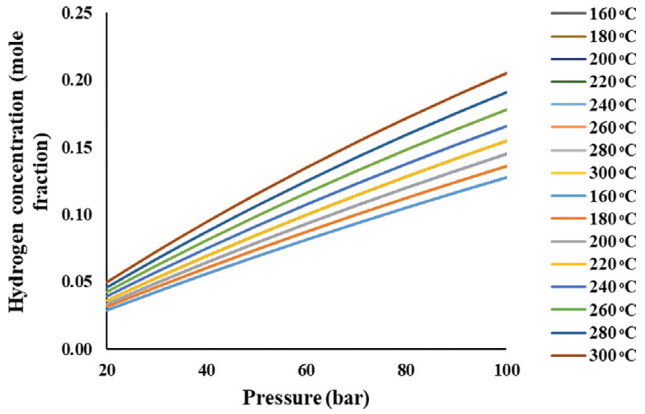

Fig. 5. Estimation of hydrogen solubility in base oil feed using NRTL model.

van't Hoff expression [39]. Under such conditions the hydrogen behaves more like liquid and hence NRTL model values were considered for liquid-phase hydrogenation. The solubility of hydrogen in base oil feed using NRTL model is reported in Fig. 5.

Based on the solubility information, the feasible region for the experimentation was decided in the range of 20 bar to 60 bar pressure and 180 °C to 220 °C temperature with due consideration given to the physical limitation of the experimental setup discussed in section 1.

2. Kinetic Experiments and Analysis

A total of thirteen different experiments were performed, out of which nine initial experiments were used for kinetic analysis in which the parameters like temperature, pressure, catalyst concentration and time were varied in the feasible region. The remaining four experiments were performed post kinetics development, out of which two were used to validate the kinetic model and two experiments were used to check the external mass transfer limitations by studying the effect of RPM on conversion. The semi-batch condition was maintained by continuously supplying hydrogen under pressure through the 450 gm of liquid pool of feed. The experimental conditions are summarised in Table 3.

The results in Table 3 suggest that the aromatics are directly converted to the nearest chemically stable molecule naphthenes, whereas the paraffins remain constant throughout the hydrogenation study. In the heterogeneous kinetic study, it is always better to check the presence of the intra-particle diffusion resistance along with the external mass transfer resistance. This helps to conceptualize the kinetic model with different transport effects and include such effects to develop a detailed kinetic model with or without these limitations [40,41].

The possible external mass transfer limitations can be evaluated by varying speed of agitation, whereas the possible limitation of intra-particle transport resistance in the heterogeneous catalytic reaction may be analyzed using the Weisz-Prater (C_{WP}) criterion [42,43]. The experimental runs 11 to 13 (in Table 3) suggest that there is no effect of the agitation on conversion, hence the absence of external mass transfer resistance in the semi-batch mode. The intra-particle diffusion limitations are separately evaluated using C_{WP} in next section.

3. Determination of Kinetic Parameters

The reaction scheme for the hydrogenation of heavy base oil is simplified as Eq. (5).

$$C_{20}H_{12}+4H_2 \rightarrow C_{20}H_{20} \quad (5)$$

The hydrogen solubility data using NRTL model suggest that the hydrogen quantity is comparable with perylene during the liquid phase hydrogenation under the semi-batch condition. The kinetic parameters were estimated by minimizing the sum of the square errors (SSE) between the experimental data points and the kinetic model using ASPEN Plus.

4. Weisz-Prater Criterion for Intraparticle Diffusion

The C_{WP} is estimated to predict whether the internal diffusion is limiting or not in the present case of heterogeneous catalytic reaction. It can be roughly defined as the ratio of reaction rate to the diffusion rate. The C_{WP} criterion states that the internal pore diffusion limitations are negligible if the Eq. (6a)-(6c) condition is satisfied [42-44].

$$C_{WP}=\frac{[-r_A]_{Obs}R^2}{D_eC_{As}}<1.0 \quad (6a)$$

$$D_e=[\varepsilon/\tau]D_{AW} \quad (6b)$$

Table 3. Experimental conditions and results for kinetic analysis

Experimental conditions	Kinetic experiments (1 to 9)									Validation runs (10 to 13)			
	1	2	3	4	5	6	7	8	9	(10)	(11)	(12)	(13)
Temperature (T), °C	220	200	200	200	200	200	190	180	180	200	220	220	220
Pressure (P), bar	60	32	30.5	30	27	24	24.5	30.5	25.5	25.5	40	40	40
Catalyst weight (W), gm	5	5	5	6	6	6	5	5	5	5	5	5	5
Time (t), hr	8	13	12	9	12	11	13	12	16	12	8	8	8
Rotor speed (rpm)	500	500	500	500	500	500	500	500	500	500	500	100	800
Results obtained													
%Aromatics (w/w)	2.98	4.77	5.00	6.10	5.60	6.30	5.60	5.75	6.42	6.04	4.76	4.76	4.76
%Naphthenes (w/w)	49.50	47.73	47.51	46.40	46.89	46.20	46.92	46.74	46.08	46.46	47.73	47.72	47.72
%Paraffins (w/w)	47.52	47.50	47.49	47.50	47.51	47.50	47.48	47.51	47.50	47.50	47.51	47.52	47.52
Conversion (X_A), fraction	0.79	0.66	0.64	0.56	0.6	0.55	0.6	0.59	0.54	0.57	0.66	0.66	0.66

$$D_{AW}=\frac{7.4\times10^{-8}T(\varphi M_W)^{0.5}}{\mu_W V_A^{0.6}} \quad (6c)$$

The C_{As} in Eq. (6a) is the concentration of aromatic solute ($C_{20}H_{12}$) on the solid catalyst surface. R is the mean radius of the catalyst particles considered as 6×10^{-4} m in the calculation. The r_A is taken as initial reaction rate for 120 minutes. The D_e in Eq. (6b) is the effective diffusivity of $C_{20}H_{12}$ in $C_{20}H_{42}$. The D_{AW} is the molecular diffusivity of $C_{20}H_{12}$ into $C_{20}H_{42}$. Several correlations are available for the calculation of D_{AW} and the Wilke-Chang correlation [45] is used in our calculations. The ε and τ in the same Eq. (6b) are the catalyst particle porosity taken as 0.43 and catalyst tortuosity factor taken as 3.56 in the C_{WP} calculation. The viscosity and other thermodynamic properties were estimated using ASPEN 10 properties package.

If $C_{WP}<<1$ then no diffusion limitations exist, and if $C_{WP}>>1$ then the internal diffusion limits the reaction [42-44]. Satterfield [46] reported that the diffusion effects will definitely be present if $C_{WP}\geq1$ and can be assumed to be insignificant when the $C_{WP}\leq0.3$. The C_{WP} for the present case was calculated to be 0.0315, suggesting that the criterion given by Satterfield is satisfied and hence the intra-particle diffusion is not a limiting factor in the present case.

5. Kinetic Modelling

The intra-particle transport limitations were neglected based on C_{WP} criterion, and the semi-batch results were fitted into different known kinetic models. The fitting suggests that the pseudo-homogeneous second-order model fits well. A two-parameter pseudo-homogeneous conversion of $C_{20}H_{12}$ (X_A) based model is given as Eq. (7a), and it is working well in the present case.

$$-r_A=\frac{dX_A}{dt}=k'C_{A0}(1-X_A)(M-X_A) \quad (7a)$$

$$M=\frac{C_{B0}}{C_{A0}}; \quad (7b)$$

$$k'=kW; \quad (7c)$$

$$k=k_0e^{-\frac{E_a}{RT}} \quad (7d)$$

In Eq. (7a), r_A is the rate of change of perylene, X_A is the conversion of perylene, and C_{A0} is initial concentration of perylene. The C_{B0} in Eq. (7b) is the initial concentration of hydrogen and ratio of C_{B0} to C_{A0} is denoted as M. The k′ in Eq. (7c) is the product of rate constant k and catalyst weight W in grams.

$$\min\left(\Sigma_{i=1}^{N_{exp}}\Sigma_{j=1}^{N_{meas}}\Sigma_{k=1}^{M_j}W_{ijk}^2(Z_j(t_{ijk})-Z_{ijk})^2\right) \quad (8)$$

The two model parameters, namely frequency factor (k_0) and activation energy (E_a), in Eq. (7d) are reported in Table 4. The values of both parameters were determined by solving a minimization problem mentioned in Eq. (8). A program in Aspen Plus was used to obtain the model parameters which is based on the least-squares method. It was used to minimize the weighted absolute square error between the observed and the predicted values of the measurements. In Eq. (8), the N_{exp} is the total number of experiments, N_{meas} is the number of measured species conversion, and M_j is the number of measurements of z(j) in i^{th} experiment.

Table 4. Kinetic parameters for the pseudo-homogeneous second-order model

Parameter	Units	Values with 95% confidence limit	Sum of square error
k_0	kmol/(m^{3}h)	31.5±0.25	0.0325
E_a	kJ/kmol	32,000±500	

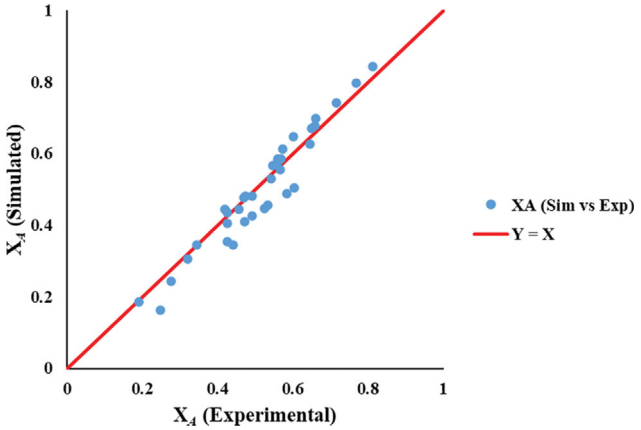

Fig. 6. Parity plot for X_A (simulated) *vs.* X_A (experimental).

The model parameters reported in Table 4 were used to estimate the conversion (X_A) and the parity plot of simulated *vs.* experimental data is shown in Fig. 6. It shows relatively good agreement between experimental and predicted results within ±15% deviation for such a complex and variable feed.

6. Validation of Kinetic Model

The parity plot presented in Fig. 6 validates the primary assumption that in absence of detailed information, the C_{20} rich base oil can be modelled using $C_{20}H_{12}$ chemical entity while mild hydrotreating the aromatic content of the selected base oil feed. We carried out two more experiments post-development of kinetics for the validation of the kinetic model. The typical trend of conversion versus time for predicted and experimental results is plotted in Fig. 7. The square error for both the validation runs is well within ±5% deviation.

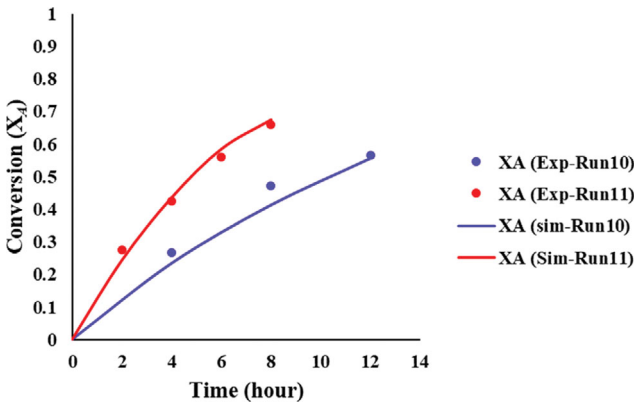

Fig. 7. Validation of developed kinetic model.

Henry and Gilbert [47] and later Satterfield [48] demonstrated that a typical conversion above 80% for hydrogenation of naphthenic lube oil can be obtained at elevated conditions. The trend of Fig. 7 reveals the slow behavior of reaction, and to achieve a conversion typically higher than 80% requires either more batch time or elevated temperature and pressure conditions. The slow nature of hydrogenation of C_{20} rich mineral base oil is due to the dilute nature of a solution.

The reason for better fitting of pseudo-homogeneous second-order kinetic model in the present case is that the specialty base oil feed exhibits a broad range of reactivity between C_{14} to C_{26}. When a large range of compounds are present and react at the rate of its respective concentration, then the overall order will be greater than one. Similar observations are reported by Henry and Gilbert [47], Weekman [49] and Mohanty et al. [50] for the typical petroleum fractions.

PARAMETRIC SENSITIVITY ANALYSIS AND KINETIC OPTIMISATION

1. Parametric Effect and Sensitivity Analysis

The experimental results of runs 1 to 11 mentioned in Table 3 were simulated as a semi-batch model in ASPEN Plus. Runs 12 and 13 were not included in the model development as the RPM has no significant effect on the conversion. The NRTL model was selected as a property package to estimate the hydrogen solubility at given experimental conditions. The kinetic parameters presented in Table 4 were provided to the semi-batch model. The conversions were estimated for the temperature range 180 °C to 300 °C, pressure range 20 bar to 100 bar and catalyst loading 5 gm to 40 gm to analyze the sensitivity of these operating conditions.

The effects of temperature, pressure and catalysts loading on the conversion are shown as 3D surface plots in Fig. 8 to Fig. 10, respectively. The effect of temperature and pressure is demonstrated by holding catalyst weight to 5 gm, whereas the effect of catalyst loading is presented by holding temperature at 200 °C. The low pressure of 20 bar obtains relatively lower conversion among all demonstrated cases of Fig. 8 to Fig. 10, suggesting the critical role of pressure. However, it is difficult to obtain the exact order of sensitivity of process variables on conversion using a 3D surface plot. To understand the order of sensitivity, a parametric sensitivity analysis was performed using PPMCC as discussed by Suryavanshi and Mohanty [51].

The PPMCC is a statistical approach to measure the bivariate correlation between the two sets of data. It is obtained by taking a ratio between the covariance of two variables and the product of

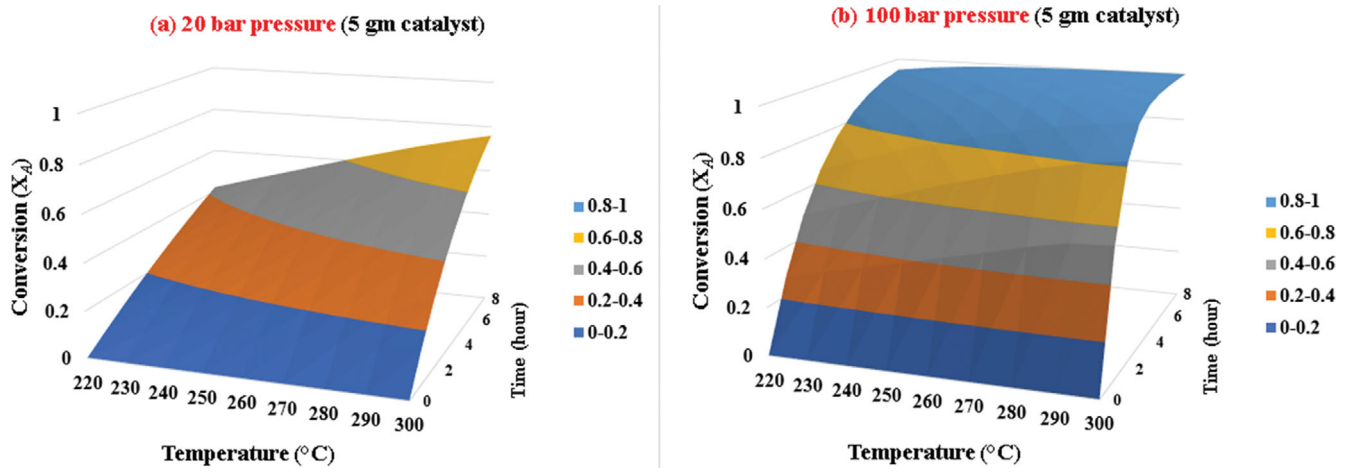

Fig. 8. Effect of pressure on conversion (a) 20 bar (b) 100 bar.

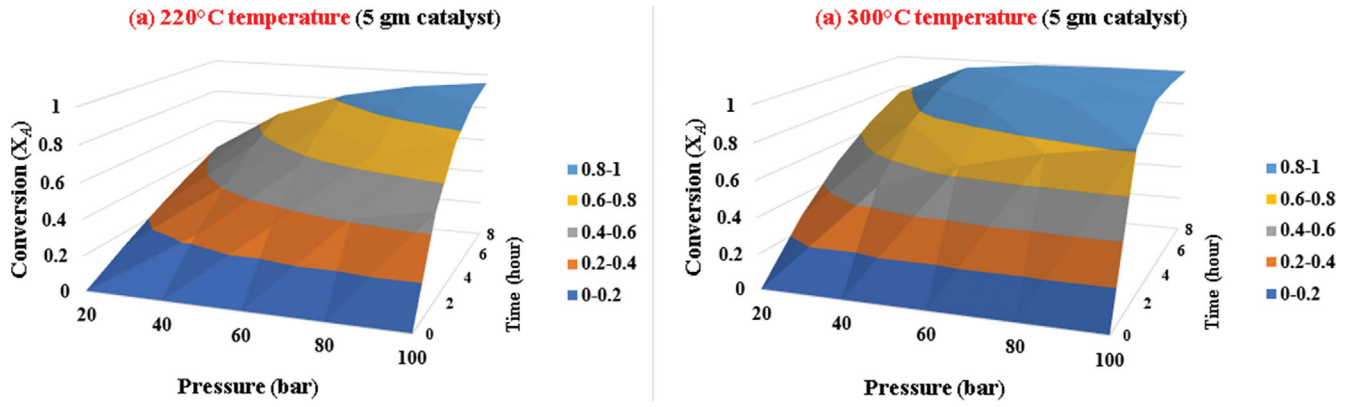

Fig. 9. Effect of temperature on conversion (a) 220 °C (b) 300 °C.

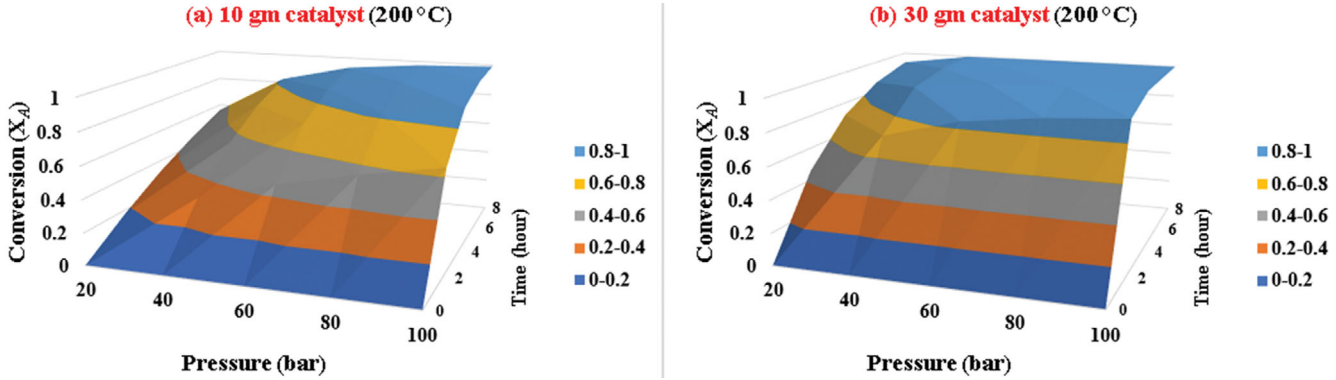

Fig. 10. Effect of catalyst loading on conversion (a) 10 gm (b) 30 gm.

(a) PPMCC matrix of variables

	T	P	W	t	Xa	
ρ =	1.0000	0.0000	0.0000	0.0000	0.3176	T
	0.0000	1.0000	0.0000	0.0000	0.4820	P
	0.0000	0.0000	1.0000	0.0000	0.3393	W
	0.0000	0.0000	0.0000	1.0000	0.4409	t
	0.3176	0.4820	0.3393	0.4409	1.0000	Xa

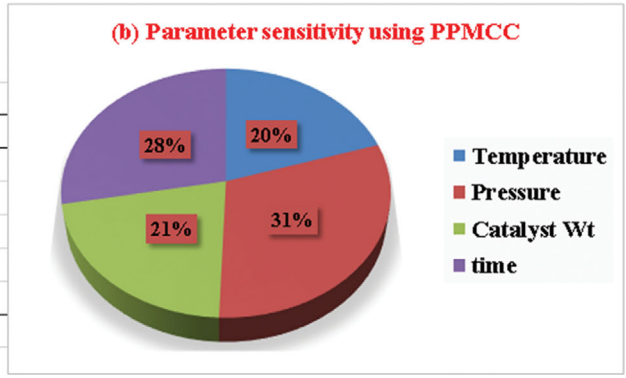

Fig. 11. Sensitivity analysis (a) PPMCC matrix (b) % sensitivity using PPMCC pie chart.

Table 5. Optimized feasible conditions for pilot scale runs

P, bar	100	100	100	100	100	100	100	100	100	100	100	100	100
T, °C	220	230	240	250	260	270	280	290	300	200	200	200	200
W, gm	5	5	5	5	5	5	5	5	5	10	20	30	40
t, hr ↓													
0	0	0	0	0	0	0	0	0	0	0	0	0	0
1	28.0	31.6	35.1	38.7	42.5	46.1	50.0	53.0	53.7	39.1	56.4	57.7	58.0
2	49.3	54.4	59.3	64.0	68.6	72.7	76.7	79.9	81.8	64.6	86.1	92.5	95.3
3	64.9	70.2	75.0	79.4	83.3	86.6	89.5	91.7	93.2	80.0	95.8	98.8	99.6
4	76.0	80.8	84.9	88.4	91.3	93.5	95.4	96.6	97.5	88.9	98.8	99.8	100.0
5	83.7	87.8	91.0	93.6	95.5	96.9	98.0	98.6	99.1	93.9	99.7	100.0	100.0
6	89.0	92.3	94.7	96.4	97.7	98.5	99.1	99.4	99.7	96.7	99.9	100.0	100.0
7	92.7	95.1	96.9	98.0	98.8	99.3	99.6	99.8	99.9	98.2	100.0	100.0	100.0
8	95.1	96.9	98.2	98.9	99.4	99.7	99.8	99.9	100.0	99.0	100.0	100.0	100.0

their standard deviations. The normalized measurement of covariance is obtained in range of −1 to +1. A PPMCC value of 0 indicates non-association between two variables. A value greater than 0 indicates positive association (increase in output with an increase in input) between variables, whereas a value less than 0 indicates negative association (decrease in output with an increase in input) between variables [51].

The results of PPMCC are shown in Fig. 11, consisting of coefficient matrix (ρ) and percentage sensitivity analysis using pie chart as Fig. 11(a) and Fig. 11(b), respectively. All coefficients of matrix ρ are positive, indicating a strong positive association between the variables. The positive values of coefficient matrix ρ suggest that all variables are sensitive and playing a significant positive role on the conversion of aromatics. The exact order of sensitivity based on Fig. 11(b) can be arranged as (P>t>W>T) on conversion, suggesting that the pressure and time are the most dominating factors in the hydrogenation of heavy base oils. The dominance of pressure can be explained on the basis of solubility of hydrogen in the liquid phase and hence pushing the reaction in forward direction. The catalyst loading and temperature are having almost simi-

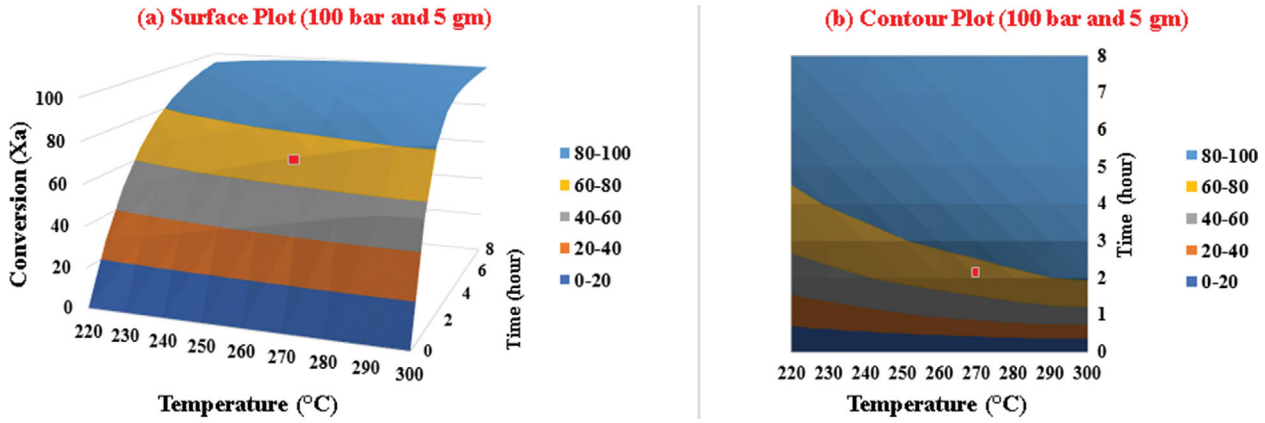

Fig. 12. Target of 70% conversion (a) 3D surface plot (b) 2D contour plot.

lar range of sensitivity towards conversion of aromatics as seen in Fig. 11(b).

2. Optimized Conditions

The set of conditions was optimized to maximize the conversion, *i.e.*, maximum AH reduced to 5% w/w or lower and ideally to 0% w/w using Aspen Plus. The pressure was observed to be the most sensitive and dominating factor, and hence it was used as fixed variable at 100 bar. The temperature, catalyst weight and time were varied between 200 °C to 300 °C, 5 gm to 40 gm and 1 hour to 8 hour respectively as reported in Table 5.

The aromatic content of the specialized base oil is required to be below 5% w/w and ideally 0% w/w (from initial concentration of 14%). Preference should be given to process conditions meeting conversion above 70% with lesser time and less catalyst requirement. The conditions meeting the conversion above 70% are highlighted in Table 5. Further, it is represented using 3D surface plot and 2D contour plot as shown in Fig. 12. Almost 100% conversion of AH could be achieved at or above 200 °C, 20 gm of catalyst loading and 5 hours of batch run. This gives a clear idea about conditions for conducting continuous experiments where the catalyst loading is much higher.

Based on these results, a pilot scale continuous experiments in a FBR at proposed condition is desirable. This would give an idea to develop an industrial scale continuous reactor. However, it is necessary to evaluate the applicability of the developed kinetic model at lab scale continuous experiments before applying to the pilot scale. Section 5 discusses the continuous experiments performed in lab-scale fixed bed reactor, and results were compared with the developed kinetic model.

CONTINUOUS FBR EXPERIMENTS

To evaluate the applicability of the developed kinetic model to continuous FBR, three additional runs were performed summarized in Table 6. The schematic of the lab-scale FBR is shown in Fig. 13. The reactor FH101 was SS 316 made having 15 cm^3 volume. It was used as FBR where the middle section (shown in grey) was filled with alumina supported Ni catalyst. The inert section of FH101 (top and bottom section) was filled with glass beads of 1.2 mm in diameter. The column diameter was 10 mm and the void space was obtained to be 60% of reactor volume.

Table 6. Experimental conditions and results for continuous FBR

Experimental conditions	Continuous FBR experiments (Lab Scale)		
	1	2	3
Temperature, (°C)	180	200	250
Pressure, (bar)	20	20	20
Catalyst loading, (gm/mL)	0.9	0.9	0.9
Base oil feed flow, (mL/min)	0.5	0.5	0.5
Hydrogen flow, (mL/min)	250	250	250
Results obtained			
%Aromatics (w/w)	8.76	8.67	4.21
%Naphthenes (w/w)	43.89	43.93	48.21
%Paraffins (w/w)	47.35	47.40	47.58
Conversion (X_A), fraction	0.374	0.381	0.699

The FBR had provision for three different streams to charge the continuous reactor. The reactant streams namely, mineral base oil stream (series 100) and hydrogen gas stream (series 200) were fed co-currently from the top under pressure. The nitrogen gas stream (series 300) was used to purge the reactor prior to the activation and before the hydrogenation. The Ni catalyst was activated by following the procedure presented in section 2.3.

After the catalyst activation, the hydrogenation was performed by operating the FBR for 5 hours (excluding purging and start-up time), in which the system achieved complete steady state after two hours. The experimental conditions and respective steady-state conversion results are reported in Table 6, which also validates that the aromatics (AH) of complex base oils are converted to naphthenes through mild hydrogenation using Ni catalyst.

A conversion of almost 70% (4.21% AH w/w) could be achieved under the pressure 20 bar, temperature 250 °C and higher catalyst loading 0.9 gm/mL. The developed kinetic model is applied for FBR simulation and the parity plot for conversion is shown in Fig. 14. The plot suggests a good agreement between simulated and experimental values for the conversion of AH. This forms the basis for the further development of a continuous process.

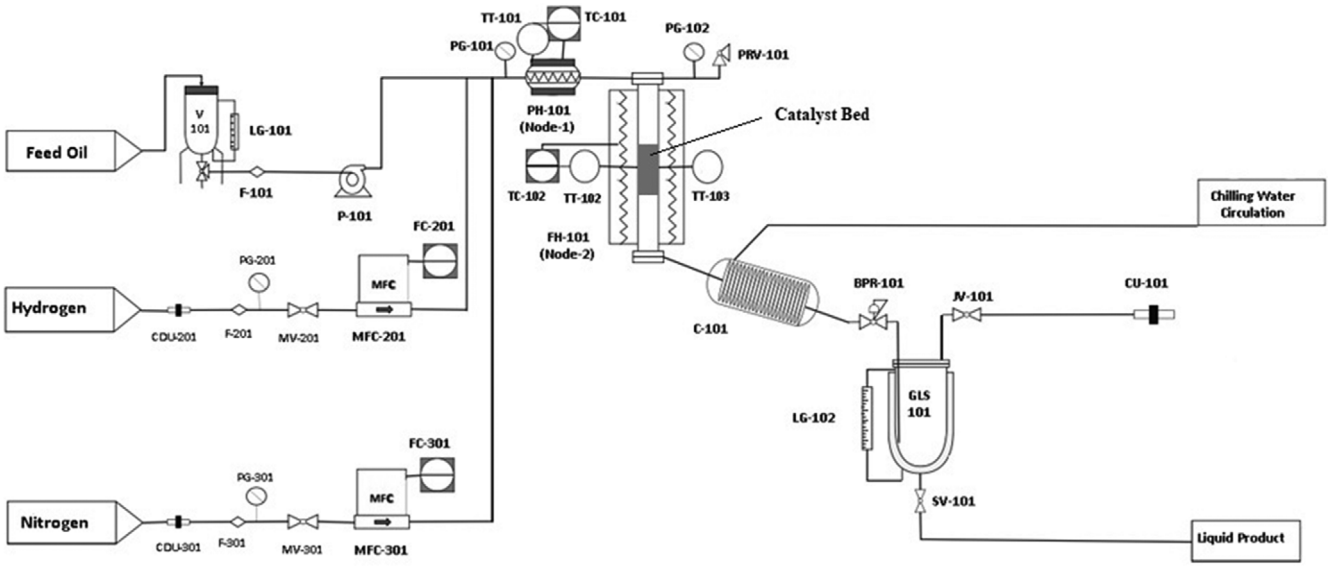

Acronym	Equipment	Acronym	Equipment
V-101	Vessel	CDU-201,301	Cylinder Discharge Unit
F-101,201,301	Flow Device	MV-201,301	Manual Valve
LG-101,102	Level Gauge	MFC-201,301	Mass Flow Controller
P-101	Pump	FC-201,301	Flow Controller
PG-101,102,201,301	Pressure Gauge	C-101	Condenser
PH-101	Pre-heater (Node-1)	BPR-101	Back Pressure Regulator
TT-101,102,103	Temperature Transmitter	GLS-101	Glass Line Separator
TC-101,102	Temperature Controller	SV-101	Sampling Valve
FH-101	Furnace Heater (Node-2)	JV-101	Jordan Valve
PRV-101	Pressure Relief Valve	CU-101	Collection Unit

Fig. 13. Schematic for Continuous FBR setup.

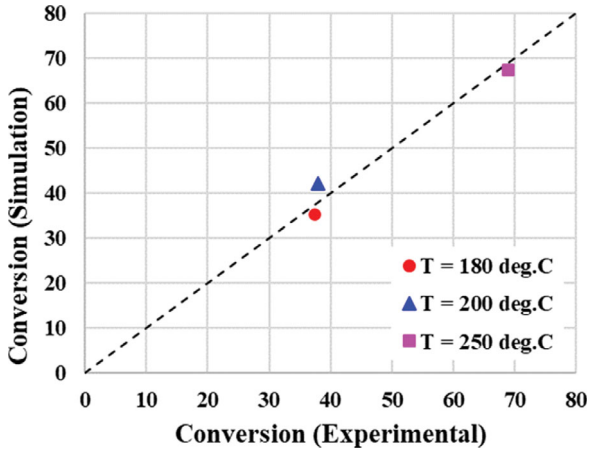

Fig. 14. Parity plot at 20 bar for continuous FBR.

CONCLUSIONS AND CRITICAL OBSERVATIONS

The current study focusses on the hydrogenation kinetics of C_{20} rich specialty base oil using an alumina-based Ni catalyst which is to be used to develop a continuous hydrogenation reactor. Following are the observations and conclusions drawn from this study.

- The solubility of hydrogen in the mineral base oil was estimated using both SRK and NRTL model; however, the values estimated using NRTL model were considered for liquid-phase hydrogenation as explained.
- The reaction occurred in a kinetically controlled regime in the range of operating conditions considered.
- The intraparticle diffusion resistance was found to be negligible based on Weisz-Prater criteria. The results also suggest the absence of external mass transfer resistance under the experimental conditions.
- The conversion was found to be influenced by pressure, residence time, catalyst concentration and temperature in the respective order.
- The pseudo-homogeneous second-order reaction kinetic model was used to obtain the kinetic parameters. The model validates the experimental data very well with the estimated kinetic parameters.
- The conditions for the complete conversion of AH were estimated for semi-batch mode.
- The developed kinetic model was used to validate the continuous FBR experiments on a lab-scale. The proposed kinetic model explains the continuous FBR experimental results very well.

ACKNOWLEDGEMENT

The authors are thankful to the Vice Chancellor of D. D. Uni-

versity, Nadiad and Managing Director of APAR Industries Limited, Mumbai, for their motivation, support and allocating of resources.

REFERENCES

1. S. Modi, M. S. Rao, T. Snigdha and T. C. S. M. Gupta, *SSRN Electron. J.*, 1 (2020).
2. T. Snigdha, S. Modi, T. Saritha, T. C. S. M. Gupta and M. S. Rao, *Proceed. Green Technol. Sustain. Dev.*, 481 (2021).
3. ASTM D-2887-13, "Standard Test Method for Boiling Range Distribution of Petroleum Fractions by GC" (June 2013).
4. A. Y. El-Nagar, R. A. El Adly, T. A. Altahli, A. Alhadhrami, F. Modather, M. A. Ebiad and A. Salem, *Pet. Sci. Technol.*, **36**(3), 179 (2018).
5. S. N. Suhaimi, A. R. A. Rahman, M. F. Md. Din, M. Z. Hassan, M. T. Ishak and M. T. Jusoh, *J. Nanomaterials*, 17 (2020).
6. *API-1509*, "API Base Oil Inter-changeability Guidelines", Annexure-E (March 2015).
7. *EU Regulation (EC) No 1223/2009* dated 30 November 2009 (published on 22 December 2009).
8. F. M. T. Luna, A. A. Pontes-Filho, E. D. Trindade, I. J. Silva, D. C. S. Azevedo and C. L. Cavalcante, *Ind. Eng. Chem. Res.*, **47**, 3207 (2008).
9. M. Busto, J. H. Sepulveda, N. R. Carrara and C. R. Vera, *Energy Fuels*, **29**(2), 1249 (2015).
10. N. Yamanaka and S. Shimazu, *Eng*, **3**, 60 (2022).
11. C. T. Tye, *IntechOpen*, *Processing of Heavy Crude Oils - Challenges and Opportunities*, Chapter-2, 1 (2019).
12. J. Gilbert and R. Kartzmark, US Patent, 3,658,692 (1972).
13. L. E. Kindwell, US Patent, 4,055,481 (1977).
14. T. Anstock, W. Himmel, M. Scharzmann, H. Dreyer, U. Lebert and A. Eisenbeis, US Patent, 4,786,402 (1988).
15. B. Corman, P. Korbach and K. Webber, US Patent, 4,801,373 (1989).
16. J. Powers, G. Prescott and J. Whiteman, US Patent, 5,855,767 (1999).
17. S. Hantzer, A. Ravella, I. Cody and D. Klein, US Patent, 6187176B1 (2001).
18. W. Lin, J. M. Chen, J. Y. Chen and K. Tsai, US Patent, 6508931B1 (2003).
19. G. R. B. Germaine, US Patent, 0258074A1 (2005).
20. J. Rosenbaum, B. Lok, K. Helling, S. Lee and R. Schexnaydre, US Patent, 8956581B2 (2015).
21. E. Kis, R. Neducin, G., Lomic, G. Boscovic, D. Z. Obadovic, J. Kiurski and P. Putanov, *Polyhedron*, **17**(1), 27 (1998).
22. H. Qin, C. Guo, Y. Wu and J. Zhang, *Korean J. Chem. Eng.*, **31**(7), 1168 (2014).
23. Z. Wei, H. Qiao, H. Yang, C. Zhang and X. Yan, *J. Alloys Compd.*, **479**, 855 (2009).
24. T. A. Le, T. W. Kim, S. H. Lee and E. D. Park, *Korean J. Chem. Eng.*, **34**, 3085 (2017).
25. J. H. Park, E. Hong, S. H. An, D. H. Lim and C. H. Shin, *Korean J. Chem. Eng.*, **34**, 2610 (2017).
26. A. Khodadadi, M. Farahmandjou and M. Yaghoubi, *Mater. Res. Express*, **6**(2), 25 (2018).
27. Y. Ghalmi, F. Habelhames, A. Sayah, A. Bahloul, B. Nessark, M. Shalabi and J. M. Nunzi, *Ionics*, **25**, 6025 (2019).
28. A. K. Sharma, S. Desnavi, C. Dixit, U. Varshney and A. Sharma, *Int. J. Chem. Eng. Appl.*, **6**(3), 156 (2015).
29. J. T. Richardson, R. Scates and M. V. Twigg, *Appl. Catl.*, **246**(1), 137 (2003).
30. J. H. Cho, S. H. An, T. Chang and C. Shin, *Catal. Lett.*, **146**, 811 (2016).
31. A. Kumar, G. D. Thakre, P. K. Arya and A. K. Jain, *Ind. Eng. Chem. Res.*, **56** (13), 3527 (2017).
32. I. Kremer, T. Tomic, Z. Katancic, Z. H. Murgic, M. Erceg and D. R. Schneider, *Clean Techn. Environ. Policy*, **23**, 811 (2021).
33. *ASTM D-6352-19E1*, "Standard Test Method for Boiling Range Distribution of Petroleum Distillates in Boiling Range from 174 °C to 700 °C by GC" (2019).
34. NIST Standard Reference Data Base, US Department of Commerce (2021). https://webbook.nist.gov/cgi/cbook.cgi?Formula=C20H12&NoIon=on&Units=SI (last accessed on October 23, 2022).
35. Report on Polycyclic Aromatic Hydrocarbons: Evaluation of sources and effects by National Research Council (US) Committee on Perylene and analogues, (Table-2.1). https://www.ncbi.nlm.nih.gov/books/NBK217758/ (last accessed on October 23, 2022).
36. Bureau of Indian Standards, *BIS: 13155 (1991)*, "Method of Test for Carbon Type Analysis of Mineral Base Oils by Infra-Red Spectrophotometry" (Reaffirmed 2001).
37. *Dow's Fire & Explosion Index Hazard Classification Guide*, 7th Ed., AIChE: New York (1994).
38. S. Modi, M. S. Rao, and T. C. S. M. Gupta, *Adv. Sustain. Dev.*, Springer Singapore, 41 (2022).
39. B. A. Schofield, Z. E. Ring and R. W. Missen, *Can. J. Chem. Eng.*, **70**(4), 822 (1992).
40. A. Singh, A. Tiwari, S. M. Mahajani and R. D. Gudi, *Ind. Eng. Chem. Res.*, **45**(6), 2017 (2006).
41. D. E. Mears, *Ind. Eng. Chem. Process Des. Dev.*, **10**(4), 541 (1971).
42. P. B. Weisz and C. D. Prater, *Adv. Catal.*, **6**(C), 143 (1954).
43. P. B. Weisz and J. S. Hicks, *Chem. Eng. Sci.*, **17**, 265 (1962).
44. L. J. Zhao and Q. Sun, *Int. J. Low-Carbon Technol.*, **10**(3), 288 (2013).
45. R. B. Bird, W. E. Stewart and E. N. Lightfoot, *Transport Phenomena*, Wiley, New York (1960).
46. C. Satterfield, *Mass Transfer in Heterogeneous Catalysis*, MIT Press, Cambridge (1970).
47. H. C. Henry and J. B. Gilbert, *Ind. Eng. Chem. Process Des. Dev.*, **12**(3), 328 (1973).
48. C. N. Satterfield, *AIChE J.*, **21**(2), 209 (1975).
49. V. W. Weekman, *Ind. Eng. Chem.*, **61**(2), 53 (1969).
50. S. Mohanty, D. Kunzru and D. N. Saraf, *Erdol & Kohle Erdgas Petrochemie*, **44**(12), 459 (1991).
51. B. Suryawanshi and B. Mohanty, *Ind. Crops Prod.*, **123**, 64 (2018).